AiMT

Advances in Military Technology
Vol. 9, No. 1, June 2014

# Effect of Impact Angle of Evaporated Particles on Behavior of Ti EB PVD Coating

D. Kottfer[1*], M. Ferdinandy[2], L. Kaczmarek[3], P. Hvizdoš[2] and M. Kuffová[4]

*[1] Faculty of Mechanical Engineering, Technical University, Kosice, Slovak Republic*
*[2] Institute of Materials Research, Slovak Academy of Sciences, Košice, Slovak Republic*
*[3] Faculty of Mechanical Engineering, University of Lodz, Łódź, Poland*
*[4] Armed Forces Academy of General Milan Rastislav Stefanik, Liptovsky Mikulas, Slovak Republic*

The manuscript was received on 21 June 2013 and was accepted after revision for publication on 20 March 2014.

**Abstract:**

*Mechanical and tribological properties of Ti coating deposited by physical vapour deposition (PVD) technique using electron beam to activate evaporation of Ti onto steel OKhN3MFA are evaluated. The thickness and grain growth direction are assessed by means of scanning with an electron microscopy, chemical composition of both the coating and substrate are measured using EDX. The coefficient of friction (COF) and wear was evaluated by a Pin-on-disc test. The wear of the coating was expressed as a loss of material (volume and mass) after the Pin-on-disc test. Hardness and Young's modulus were found to be from 3.8 GPa to 7.6 GPa and from 65 GPa to 200 GPa, respectively. The measured values of the studied properties were compared with the literature data for Ti PVD coatings.*

**Keywords:**

*Evaporation, EB PVD, hardness, coefficient of the friction, wear*

## 1. Introduction

Coatings on surfaces of mechanical components are formed:

- With an aim to improve mechanical properties, e.g. hardness [1-4], adhesion [4, 5] and tribological properties [6-8], e.g. COF and wear resistance. Several combinations of reactive elements were tested, including Ti/C,N [1], Cr,Al/N

* *Corresponding author: Daniel Kottfer, Department of Technology and Materials, Faculty of Mechanical Engineering, Technical University of Kosice, Mäsiarska 74, 040 01 Kosice, Slovak Republic, phone: +421 55 602 35 10, fax: +421 55 622 51 86, E-mail: daniel.kottfer@tuke.sk*

[2, 3], Ti,AlCr/N [6-8]. Ti based coatings are widely used as hard, low friction, and wear resistant protective layers [1-4]. Yanhui Zhao et al. studied properties of TiN/TiC multilayer films deposited by pulse biased arc ion plating. They found hardness of TiN and TiC coatings to be (25.2 ± 2.8) GPa and (27.4 ± 3.2) GPa, respectively [1]. Thickness of investigated TiN and TiC coatings were 2.01 μm and 2.45 μm, respectively [1]. Yasuo Tanno and Akira Azushima studied the effect of counterpart materials on COF of TiN coatings with preferred grain orientations. They measured hardness of TiN(111) and TiN(200) coating equal to (25.1 ± 1.6) GPa and (21.1 ± 0.5) GPa, respectively [4]. In both cases, there was a critical scratch load of about 50 N [4]. In both cases, the COF equaled 0.2 for $Al_2O_3$ and WC-Co ball as counterpart [4].

- With an aim to increase corrosion resistance [8, 9] and cutting properties [6-8, 10] of cutting tools, Fox-Rabinovich et al. studied tribological adaptability of TiAlN and TiAlCrN PVD coatings under high performance dry machining (milling) conditions. They found that the best tool life is that of the coating with highest amount of $Ti_{0.10}Al_{0.20}Cr_{0.70}N$. This coating has twice better tool life in comparison to the TiAlN coating [7].

Ti coatings have low hardness, high COF, and therefore they are not usually used as functional layers. On the other hand, Ti coatings have good adhesion and appropriate thermal expansion, that is why they are often used as interlayers to improve adhesion of the protective layers [10, 17, 20-22, 25]. Properties of Ti coatings have been studied extensively [10, 12, 14-25].

T. Jamal et al. [10] evaluated friction and adhesive wear of titanium carbide and titanium nitride overlay coatings, where measured hardness and COF of Ti interlayer equaled 2.255 GPa and 0.765, respectively.

S. Kataria et al. [14] studied selected mechanical properties of Ti thin films deposited by magnetron sputtering PVD technique on D9 steel. The film hardness measured at the surface of the coatings exhibited a value of 2.5 GPa. Adhesion (critical load to failure) for this coating was evaluated at 2 N.

S. Kataria et al. [15] evaluated tribological and deformation behavior of titanium coating under different sliding contact conditions. Three different loads of 1N, 3N and 9N and three different speeds 0.1, 0.5, and 2.0 cm/s were used at each load to study the effect of speed on the tribological behavior of Ti coating. The counterparts were $Al_2O_3$, $Si_3N_4$ and steel balls with a diameter of 6 mm. A tribometer (CSM Instruments, Switzerland) was used in linear reciprocating mode to carry out frictional tests. The COF, roughness and hardness of the deposited Ti coatings were 0.7 (for steel ball as counterpart); 38.5 nm and 2.5 GPa, respectively

N. Chelliah and S.V. Kailas [16] studied synergy between tribo-oxidation and strain rate response on governing the dry sliding wear behaviour of titanium where presented values of Ti: hardness and Young’s modulus 1.65 GPa and 104 GPa, respectively. Three loads 15.3 N, 45.8 N and 76 N were used, and five sliding speeds 0.05 m/s, 0.1 m/s, 0.45 m/s, 1.0 m/s, and 1.4 m/s were used. The sliding distance was 1500 mm. COF values were from 0.39 upwards.

B. Bhushan and B. K. Gupta in [17] presented values of hardness and COF of Ti coating equal to 2.255 GPa and 0.8, respectively.

N. Randall in [18, 19] reported values of hardness and Young’s modulus of Ti coating equal to 16 GPa and 270 GPa, respectively.

J. Xu et al. [20] studied the structure, hardness and Young's modulus of Pd/Ti nanostructured multilayer films, where measured hardness and Young's modulus of Ti interlayer were 8.6 GPa and 150 GPa, respectively.

G. S. Kim et al. [21] investigated the effects of the thickness of Ti buffer layer on the mechanical properties of TiN coatings. Hardness and Young's modulus were 8.2 GPa and 220 GPa, respectively.

A. A. Voevodin et al. [22] evaluated the design of a Ti/TiC/DLC functionally gradient coating based on studies of structural transitions in Ti–C thin films. Ti coating was prepared by a hybrid of magnetron sputtering and pulsed laser deposition. They measured the value of hardness and Young's modulus of Ti interlayer equal to 4 GPa and 175 GPa, respectively.

K. Miyoshi et al. [23] studied sliding wear and fretting wear of diamond like carbon-based, functionally graded nano composite coatings. Hardness and Young's modulus of 50 nm thick Ti interlayer deposited onto AISI 440C stainless steel were 4 GPa and 140 GPa, respectively.

K. Chu et al. [25] evaluated the structural and mechanical properties of titanium and titanium diboride monolayers and Ti/TiB2 multilayers. They measured hardness and Young's modulus of Ti interlayer 12.5 GPa and 185 GPa, respectively.

The aim of this paper is to determine the tribological properties of the hard, Young's modulus, adhesion, COF and wear resistant, thin Ti coating obtained in the EB PVD process on the OKhN3MFA steel for various angles of incidence of evaporated Ti particles with the surface that was being coated. This Ti coating was tested by selected methods. These methods are in correlation, and together they can give us information about the quality of the applied coating. The next aim of the paper is to compare the measured values of material properties with results of above-mentioned authors.

## 2. Preparation of Specimens and Experimental Procedure

Experimental samples were prepared from OKHN3MFA steel (chemical composition is in Table 1). Before, deposition substrates were mechanically polished to a surface roughness of $R_a$ equal to 0.40 μm to 0.60 μm and annealed (in Ar protective atmosphere) at 400 °C in order to remove the residual stresses. The samples for coating thickness measured by means of observing the brittle fracture were further shaped for easy fracturing. Their dimensions were as follows: the length – 35 mm, the width – 6 mm and the height – 5 mm. A sharp V-notch was made in them (Fig. 1) by Electro spark cutting. The evaluated coating was at the tensile surface of the bar. The samples for tribological testing were prepared according to the standard requirements for Pin-on-disc testing (Fig. 2). Their dimensions were 50 mm diameter, and 5 mm thickness (Fig. 2). Micro-hardness and Young's modulus were measured on the same samples.

*Tab. 1 Chemical composition of OKhN3MFA steel substrates (ZTS Matec, Slovakia, producer)*

| Element | C | Mn | Si | Cr | Ni | Mo | S | P | Cu | Sb | V |
|---|---|---|---|---|---|---|---|---|---|---|---|
| mass [%] | 0.36 | 0.50 | 0.25 | 0.82 | 2.87 | 0.30 | 0.004 | 0.014 | 0.15 | 0.007 | 0.12 |

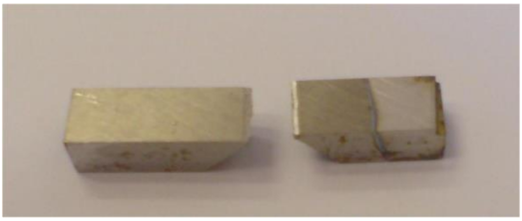

*Fig. 1 Sample for evaluation of Ti coating thickness with V-notch after its fracture.*

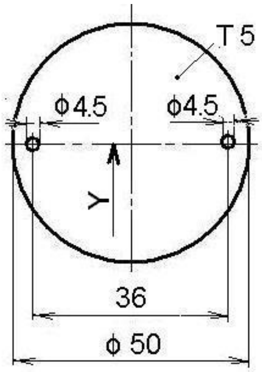


*Fig. 2 Shape of the sample for the Pin-on-disc test, T5 – thickness of sample, Y – distance, measured thickness of the coating*

Ti coating was deposited by activated evaporation by electron beam EB PVD (Fig. 3) according to parameters [14] shown in Table 2. Only one sample surface was exposed and distances of the samples from crucible with evaporated Ti (height *Y*) were 305 mm, 335 mm, 365 mm, and 425 mm, distance from the axis perpendicular to the crucible surface (distance *X*) was 120 mm (Fig. 4). The samples were located in accordance with Fig. 4, height *Y* being across the sample's fracture (Fig. 1) and being across the center of sample for Pin-on-disc test (axis marked by arrow, Fig. 2). All coatings were deposited within one process cycle. The placing of the samples in the vacuum chamber was such that all the above mentioned properties together with grain growth angle $\alpha$ in dependence on the angle of incidence of the evaporated Ti particles $\beta$ were included. In the present geometry this angle was 12° to 23.5°. Power of electron gun was 2.5 kW, cathode current was 0.2 A, ARE electrode voltage was 240 V and coating deposition time was 30 min. The pressure inside the vacuum chamber during the deposition was 0.01 Pa.

Before, deposition substrates were cleaned by ultrasound in acetone and subjected to Ar plasma etching: $P$ = 0.2 Pa, $U$ = 1.2 kV, $t$ = 20 min and heating: $P$ = 5 Pa, $U$ = 1.24 kV, $t$ = 60 s.

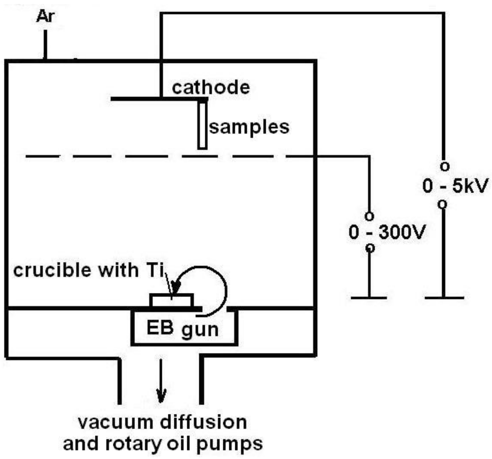


*Fig. 3 The apparatus for activated evaporation using electron beam (EB PVD), schematically*

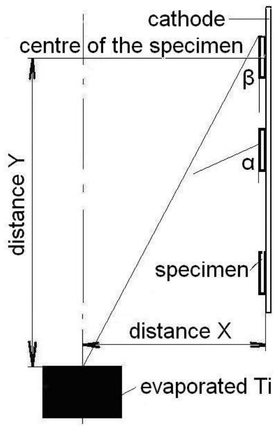


*Fig. 4 Locations of samples inside the vacuum chamber, schematically*

*Tab. 2 Main process parameters for the Ti coating deposition*

| Coating | Technique | Pressure [Pa] | Temperature [°C] | $I_{catode}$ [A] | $U$ [V] |
|---|---|---|---|---|---|
| Ti | EB PVD | 0.01 | 200 | 0.2 | 240 |

The thickness (Fig. 5, 6) and chemical compound (Tab. 4) of investigated coatings and substrate were determined by the scanning electron microscope Jeol JSM 7000F and EDX analysis. The thickness was measured on the brittle fracture made after cooling down the sample in liquid nitrogen. The samples were cleaned by ultrasonication in organic solvent for 5 min and then were dried by blowing warm air for 3 min.

Grain growth direction – angle $\alpha$ – of layer was evaluated by observing the brittle fracture (Fig. 5, 6) in the scanning electron microscope (SEM) Jeol JSM 7000F.

The surface roughness investigations of samples and deposited coatings were made on the Surftest SJ-310 MITUTOYO device at temperature 22 °C.

The micro-hardness tests of coatings were made on the CSM Ultra-micro-hardness tester. Test conditions were selected so that the penetration depth was a maximum of 0.1 of the thickness of evaluated coatings, eliminating influence of the substrate on the measurement results. Values of penetration depth were up to 70 nm. Measurements were made using Berkovich indenter with sinus load mode at frequency of loading 20 Hz. The peak load was 0.07 N. This technique allows calculating the depth profile of hardness and Young's modulus.

Tribological tests were carried out on the CSM "Pin-on-disc" tester with the following conditions: the counter-specimen ball made from the 100Cr6 steel ball with the 6 mm diameter, the load was 0.5 N, the friction radius was 5 mm, the linear velocity was 15 cm/s, the overall sliding distance was 100 m and the ambient temperature was 22 °C. Wear trace of the 100Cr6 steel ball was situated into the center of the specimen in order to ensure the equal thickness of measured coating (Fig. 2) for track radius of 5 mm. The character of the developed failure was evaluated based on observations from the Olympus GX 71 light microscope. The wear was expressed in terms of volume loss during the wear test. For the cross section of the wear track, a Surftest 301 Stylus by Mitutoyo was used. From the measured friction force COF was calculated. By multiplying the calculated volume by the Ti density, the mass of the lost material was found.

The volume loss was calculated as follows: The cross section area of the wear track was found from graphical record made by the profiler (Fig. 10). The volume was then calculated as:

$$V = Sl \tag{1}$$

where $V$ is the volume of the wear track – volume loss ($mm^3$), $S$ is the cross section area ($mm^2$), $l$ is the length of the wear circle made by counterpart (steel ball) $l = 2\pi r$, (mm), $r$ is the radius of the wear circle (mm).

*Tab. 3 Parameters of Pin-on-disc testing*

| Sample | Distance $Y$ [cm] | Thickness of Ti coating [μm] | Radius of track [mm] | Sliding speed [cm/s] | Sliding distance [m] | Load [N] |
|---|---|---|---|---|---|---|
| 1 | 30.5 | 6.85 | 5 | 15 | 100 | 0.5 |
| 2 | 36.5 | 2.57 | | | | |
| 3 | 42.5 | 1.60 | | | | |

## 3. Results and Discussion

The coating thickness and its distribution along the surface are in a good agreement with [12]. The values of thickness were from 1.6 μm to 6.85 μm (Fig. 5, 6). Chemical composition of the Ti coating (Tab. 4) as measured by EDX showed (Fig. 7) that the coating contains Fe, in addition to Ti, where the Fe signal comes from the substrate due to the size of the volume excited by incident electrons.

The column of the Ti coating grew with inclination $\alpha$ (Fig. 4), measured with respect to the coated surface. The values of $\alpha$ were from 45° to 60° (Tab. 5), which with respect to the impact angle $\beta$ from 12° to 23.5° can be considered suitable. The values of the angle $\alpha$ grew with distance H and thus with the impact angle $\beta$. Angle $\alpha$ was 60° for $\beta$ = 23°, i.e. for Y 305 mm and 335 mm.

Roughness $R_a$ of the coating was from 0.42 μm to 0.49 μm for substrate with the roughness of 0.42 to 0.47 μm, which shows that the PVD coating followed the roughness of the substrate. Occasional deviation of the roughness of the Ti coating from the values for substrate could be influenced by local irregularities of the coating.

Hardness and Young's modulus of the Ti coating were carried out on CSM Instruments equipment according to the ISO 14577 International Standard. Each hardness value is a mean of 5 to 10 measurements. For the coating hardness the maximum measured value was taken. The measured hardness was from 3.8 GPa to 7.6 GPa. The maximum hardness, 7.6 GPa, was achieved for Ti coating made for $Y$ = 305 mm and 335 mm. On the other hand, the lowest value, 3.8 GPa, was found for $H$ = 425 mm (Fig. 9). The maximum value is 3 to 4 times higher than those reported in [10, 14, 16, 17], it is 90 % higher than that in [22, 23], it agrees with [18, 19], it is 60 % lower than that in [25] and 110 % lower than in [20, 21]. The lower values found in our study could be caused by lower densities of columnar grains and defects of the coatings such as pores and surface irregularities due to roughness ($R_a$ from 0.4 μm to 0.6 μm). Higher roughness (uneven surface features such as micro-drops) can affect the process of indentation – imperfect tip-surface contact, incorrect identification of contact – all that can result in much greater apparent depth of penetration and thus significantly lower measured values of hardness and Young's modulus.

Young's moduli of Ti coatings were found in a similar way. Each value is an average of 5 to 10 measurements. The measured values of Young's modulus were 65 GPa to 200 GPa. The maximum value is close to those in [20, 21, 25], 90 % higher than in [16], 25 % higher than in [23] and 35 % lower than reported in [18, 19].

COF was found under the conditions presented in Table 3. After a short run-up phase, the COF values increased to 0.3, then grew linearly up to 0.4 in cases of samples 2 and 3 until the sliding distance of 50 mm (Fig. 12). For sample No. 2, COF increased rapidly to a value close to 0.85, which subsequently varied slightly up to the maximum of 0.93 which remained stable for the duration of the testing distance (Fig. 12). This value is about 15 % higher than that found by Bhushan and Gupta ($\mu$ = 0.80) [17]. The sharp increase of COF could be caused by the movement of a significant amount of Ti debris towards the rims of the wear track, which significantly increased the contact area between the ball and Ti coating. Final depth of the wear track did not exceed the Ti coating thickness (Fig. 11).

In the case of sample No. 3, COF grew linearly up to approximately 0.4 at 60 mm distance. It then started to increase rapidly up to the maximum of 0.63, which remains stable until the end of the sliding distance. This value is 50 % higher than that in [16], and 10 % ÷ 30 % lower than those in [10, 15, 17]. The cause of the rapid increase of COF could be – similarly as in the sample 2 – the transfer of part of the Ti material towards the track rim, thus enlarging the contact area. However, the final depth of the wear track was higher than Ti coating thickness (Fig. 11). This means that also wear of the steel substrate took place. In the case of sample No. 1, the COF development was linear, growing from the initial 0.3 up to 0.6. After a movement of 90 mm, the increase of COF was more rapid and by the end of the test it reached 0.84. This is an acceptable result [5]. In this case, no significant transfer of material to the wear track rims occurred. This is also the reason why COF grew linearly, the wear of the coating increased with sliding distance. The rapid and linear increasing trend toward the end of the test indicates that rapid wear of the coating was taking place but no damage of the substrate occurred (Fig. 11).

Wear was evaluated as mass loss after the wear testing. This mass loss for samples 1, 2 and 3 were 6.862 mg, 7.564 mg and 6.013 mg (Tab. 6), respectively. Sample 3 suffered the lowest wear with the smallest thickness of 1.2 μm. On the other hand, the damage of the substrate occurred, which is visible as lighter colored surface in the wear track (Fig. 14). More intense wear was observed in the thickest Ti coating of 6.85 μm. These results correspond to the width of the wear tracks after Pin-on-disc test (Figs 13, 14). The most worn was the Ti coating No. 2 with minimum thickness 3.2 µm. Wear of the steel ball was directly proportional to the thickness of the tested Ti coating (Tab. 6).

*Tab. 4 Chemical compound of Ti coating*

| Element | Mass [%] | Atomic [%] |
|---|---|---|
| Ti | 91.97 | 93.03 |
| Fe | 8.03 | 6.97 |
| Totals | 100.00 | 100.00 |

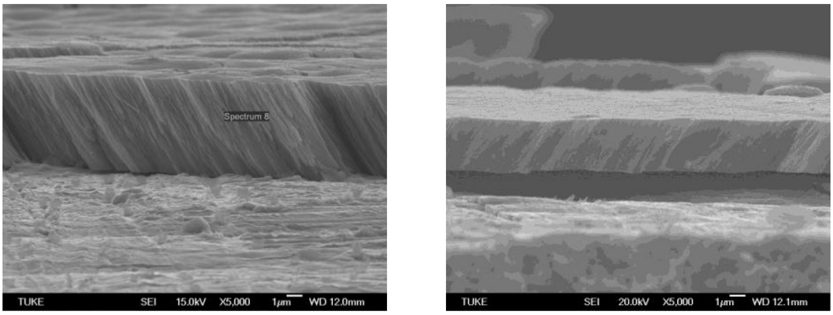


*Fig. 5 Thickness of Ti coating: Y = 305 mm (left) and Y = 335 mm (right), distance X = 120 mm*

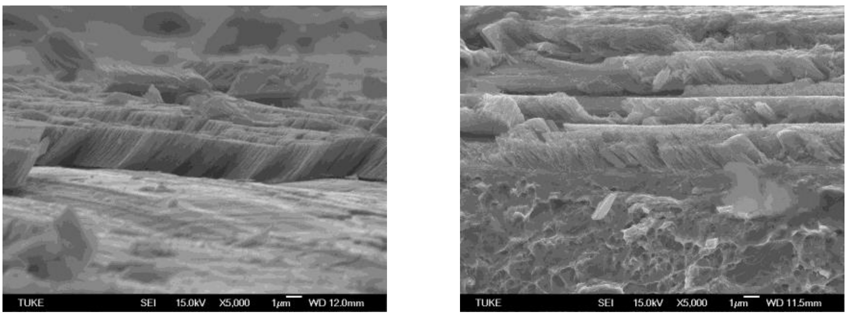


*Fig. 6 Thickness of Ti coating: Y = 365 mm (left) and Y = 425 mm (right), distance X =120 mm.*

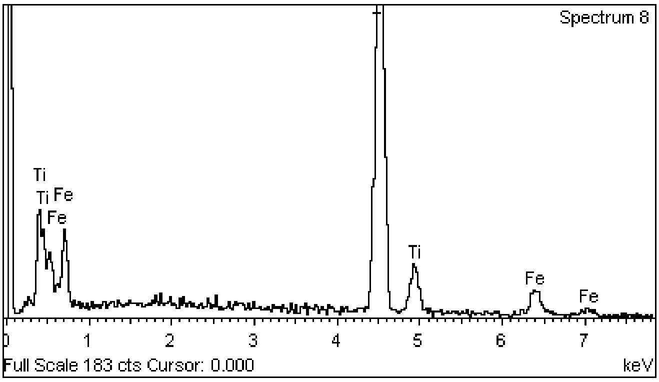


*Fig. 7 EDX of the Ti coating*

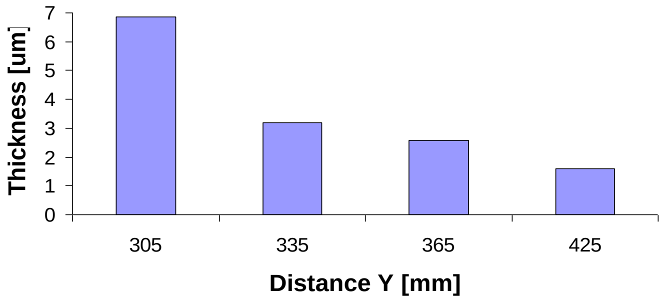


*Fig. 8 Thickness of Ti coating as function of height Y above crucible with evaporated Ti, distance X = 120 mm.*

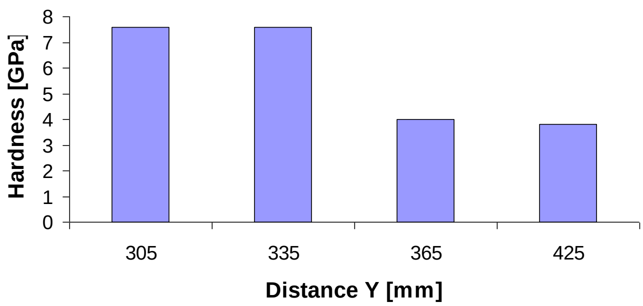


*Fig. 9 Hardness as function of Y, distance X=120 mm*

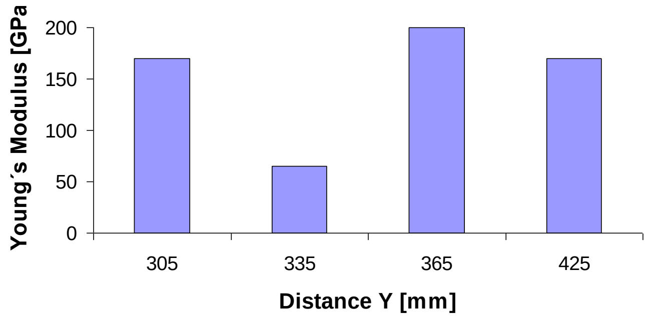


*Fig. 10 Dependence of Young's modulus on the distance Y, distance X = 120 mm*

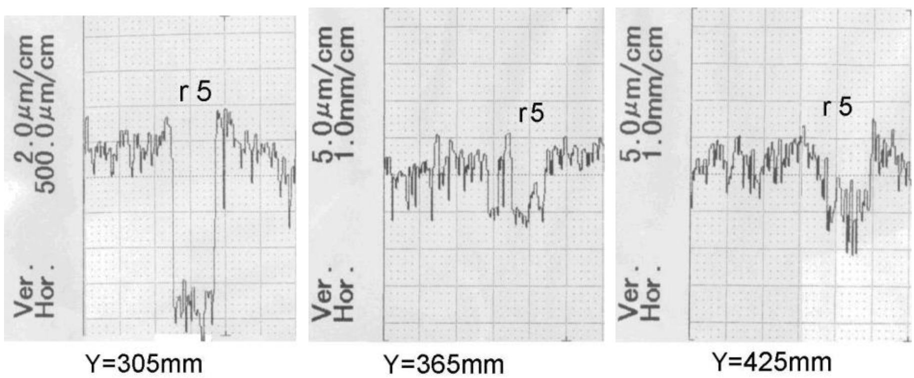


*Fig. 11 Profiler records corresponding to cross section of the wear tracks: Sample 1: Y = 305 mm, sample 2: 365 mm, and sample 3: 425 mm, X =120 mm*

*Tab. 5 Measured values of Ti grain growth angle α as function of target-cathode distance Y, X = 120 mm*

| Distance *Y* [mm] | 305 | 335 | 365 | 425 |
|---|---|---|---|---|
| Angle $\alpha$ [°] | 60 | 60 | 50 | 45 |

*Table 6 Measured values of wear of Ti coating worn against steel ball*

| Sample | Distance *Y* [mm] | Wear of the coating [mg] | Wear of ball [mg] | Dimensions of the ball worn cap [mm] |
|---|---|---|---|---|
| 1 | 305 | 6.862 | 11.11 | 0.874 × 0.663 |
| 2 | 365 | 7.564 | 8.433 | 0.515 × 0.512 |
| 3 | 425 | 6.013 | 1.044 | 0.484 × 0.370 |

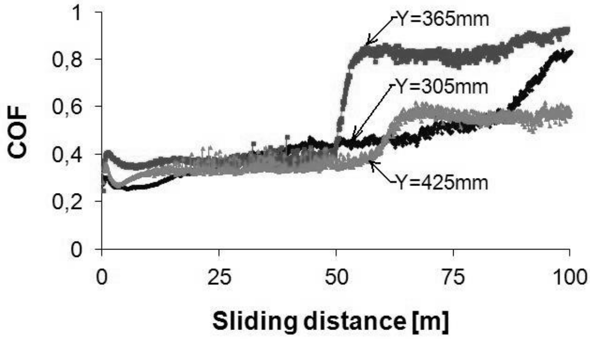


*Fig. 12 Development of the COF along the sliding distance, X =120 mm*

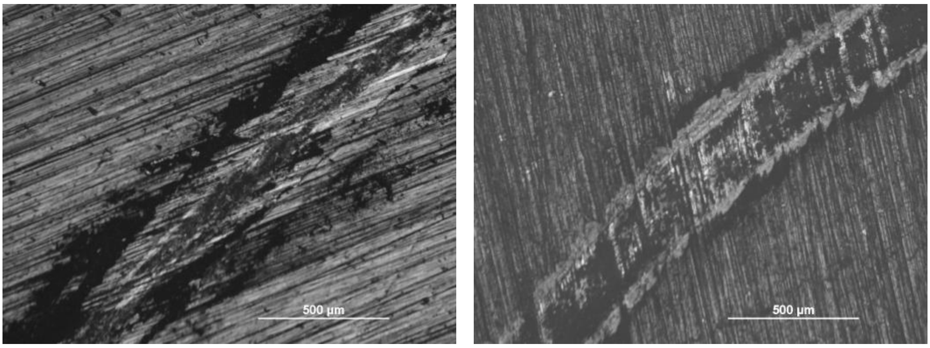


*Fig.13 Wear tracks after Pin-on-disc testing of Ti coatings: sample No. 1 (left): Y = 305 mm, sample No. 2 (right): Y = 365 mm, X =120 mm*

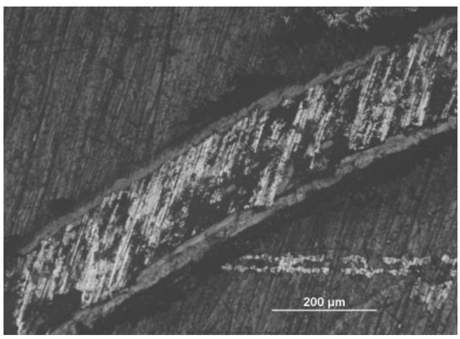


*Fig. 14 Wear track, sample No. 3: Y = 425 mm, X =120 mm*

## 4. Conclusions

According to the measurements and analyses, the following conclusions can be drawn:

- Properties such as coating thickness, Ti grain growth direction, hardness, Young's modulus, COF, and wear of Ti coatings deposited on 0KhN3MFA (GOST) steel substrates were experimentally evaluated.
- These properties were measured for coatings prepared on four different places above the crucible with evaporated Ti with distances $Y$ = 305 mm, 335 mm, 365 mm, and 425 mm. The sideways distance $X$ was 120 mm.
- Thickness of Ti coatings for the distances $Y$ 305 mm, 335 mm, 365 mm and 425 mm was 6.85 µm, 3.27 µm, 2.57 µm and 1.6 µm, respectively.
- The Ti coating has a columnar microstructure, angle of the Ti grain growth direction $\alpha$ reached values 40° to 60°, which can be considered as acceptable with respect to the incident angle $\beta$ from 12° to 28°.
- Measured values of hardness were 7.6 GPa, 7.6 GPa, 4.0 GPa and 3.8 GPa. Maximum value 7.6 GPa was reached by the coating prepared for $Y$ = 305 mm and 335 mm. The lowest hardness 3.8 GPa was found for $H$ = 425 mm. Maximum hardness is 3 to 4 times higher than that in [10, 14, 16, 17], it is 90 % higher than that in [22, 23], agrees with [18, 19], it is 60 % lower than in [25] and 110 % lower than those reported in [20, 21]. The lower values can be caused by lower density of the columnar grains and potential defects of coatings (irregularities due to higher roughness – $R_a$ were from 0.42 to 0.49 µm).
- The Young's moduli were from 65 GPa to 200 GPa (Fig. 10). The maximum value is close to those found in [20, 21, 25], it is 90 % higher than in [16], 25 % higher than in [23] and 35 % lower than those reported in [18, 19].
- COF was measured in dry sliding under conditions summarized in Tab. 3. For samples 1, 2 and 3, COF was 0.84, 0.92 and 0.62, respectively. These values are in agreement with [10, 15, 17] and 50 % to 10 % higher than those in [16].
- Wear was expressed in terms of mass loss during the Pin-on-disc test. These losses were for samples 1, 2 and 3 and were equal to 6.862 mg, 7.564 mg and 6.013 mg, respectively. In the case of samples 1 and 2, the depth of the wear tracks was smaller than the coating thickness. In the case of sample 3, this depth exceeded the Ti coating thickness.

## References

[1] ZHAO, Y., LIN, G., XIAO, J., DONG, CH. and WEN, L. TiN/TiC multilayer films deposited by pulse biased arc ion plating. *Vacuum*, 2010, no. 85 p. 1-4.

[2] ENDRINO, JL. and DERFLINGER, V. The influence of alloying elements on the phase stability and mechanical properties of AlCrN coatings. *Surface & Coatings Technology*, 2005, no. 200, p. 988-992.

[3] TLILI, B., MUSTAPHA, N., NOUVEAU, C., BENLATRECHE, Y., GUILLEMOT, G. and LAMBERTIN, M. Correlation between thermal properties and aluminium fractions in CrAlN layers, deposited by PVD technique. *Vacuum*, 2010, no. 84, p. 1067-1074.

[4] TANNO, Z. and AZUSHIMA, A. Effect of counter materials on coefficients of friction of TiN coatings with preferred grain orientations. *Wear,* 2009, no. 266, p. 1178-1184.

[5] PAKUŁA, D., DOBRZANSKI, LA., GOŁOMBEK, K., PANCIELEJKO, M. and KŘIŽ, A. Structure and properties of the $Si_3N_4$ nitride ceramics with hard wear resistant coatings. *Journal of Materials Processing Technology,* 2004, no. 157-158, p. 388-393.

[6] FOX-RABINOVICH, GS., YAMAMOTO, K., VELDHUIS, SC., KOVALEV, AI. and DOSBAEVA, GK. Tribological adaptability of TiAlCrN PVD coatings under high performance dry machining conditions. *Surface & Coatings Technology*, 2005, no. 200, p. 1804.

[7] WENDLER, B., KACZMAREK, Ł., KLIMEK, L., RYLSKI A. and JACHOWICZ M. Nanocrystalline - TiAl based microalloyed coatings as gas corrosion barriers. *Reviews on Advanced Materials Science*, 2004, no. 8, p. 116-121.

[8] CAICEIRO, JC., CABRERA, G., CAICEIDO, HH., AMAYA, C. and APERADOR, W. Nature in corrosion-erosion surface for [TiN/TiAlN]n nanometric multilayers growth on AISI 1045 steel. *Thin Solid Films*, 2012, no. 520, p. 4350-4361.

[9] KOVALEV, AI., WAINSTEIN, DL., RASHKOVSKIY, AY., FOX-RABINOVICH, GS., YAMAMOTO, K., VELDHUIS, S., AGUIRRE, M. and BEAKE, BD. Impact of Al and Cr alloying in TiN-based PVD coatings on cutting performance during machining of hard to cut materials. *Vacuum*, 2010, no. 84, p. 184-187.

[10] JAMAL, T., NIMMAGADA, R. and BUNSHAH, RF. Friction and Adhesive Wear of Titanium Carbide and Titanium Nitride Overlay Coatings. *Thin Solid Films*, 1980, no. 73, p. 245-254.

[11] PERZYNSKI, K., MAJOR, Ł., MADEJ, Ł. and PIETRZYK, M. Analysis of the Stress Concentration in the Nanomultilayer Coatings Based on Digital Representation of the Structure. *Archives of Metallurgy and Materials*, 2011, vol. 56, no. 2, p. 393-399.

[12] MATTHEWS, A. and LEFKOW, AR. Problems in the physical vapour deposition of titanium nitride. *Thin Solid Films*, 1985, no. 126, p. 283-291.

[13] KOTTFER, D. *Thin coatings on internal cylindrical surfaces* (in Slovak), [Habilitation thesis]. Technical University of Košice, Faculty of Mechanical Engineering, 2010, p. 92.

[14] KATARIA, S., RAMASESHAN, R., DASH S. and TYAGI, AK. Nanoindentation and Scratch Studies on Magnetron Sputtered Ti Thin Films. *J. Nanosci. Nanotechnol.*, 2009, no. 9, p. 5476-5479.

[15] KATARIA, S., KUMAR, N., DASH, S. and TYAGI, AK. Tribological and deformation behaviour of titanium coating under different sliding contact conditions. *Wear,* 2010, no. 269, p. 797-803.

[16] CHELLIAH, N. and KAILAS, SV. Synergy between tribo-oxidation and strain rate response on governing the dry sliding wear behaviour of titanium. *Wear*, 2009, no. 266, p. 704-712.

[17] BHUSHAN, B. and GUPTA, BK. *Handbook of tribology*, McGraw-Hill Inc., 1991, p. 1069. ISBN 0-07-005249-2.

[18] RANDALL, NX. Finer particle size allows better coating characterisation with the Calotest, *Applications bulletin*. Document AB No5, CSM Instruments, Advanced Mechanical Surface Testing, October 1997.

[19] RANDALL, NX. *Development and application of a multifunctional nanotribological tool.* [PhD thesis] University of Neuchâtel, Switzerland, 1997

[20] XU, J., KAMIKO, M., SAWADA, H., ZHOU, Y., YAMAMOTO, R., YU, L. and KOJIMA, I. Structure, hardness, and elastic modulus of Pd/Ti nanostructured multilayer films. *J. Vac. Sci. Technol.,* B 21.6., Nov-Dec 2003.

[21] KIM, GS., LEE, SY., HAHN, JH., LEE, BY., HAN, JG., LEE, JH. and LEE, SY. Effects of the thickness of Ti buffer layer on the mechanical properties of TiN coatings. *Surface and Coatings Technology,* 2003, no. 171, p. 83-90.

[22] VOEVODIN, AA., CAPANO, MA., LAUBE, SJP., DONLEY, MS. and ZABINSKI, JS. Design of a Ti/TiC/DLC functionally gradient coating based on studies of structural transitions in Ti-C thin films. *Thin Solid Films,* 1997, no. 298, p. 107-115.

[23] MIYOSHI, K., POHLCHUCK, B., STREET, KW., ZABINSKI, JS., SANDERS, JH., VOEVODIN, AA. and WU, RLC. Sliding wear and fretting wear of diamond like carbon-based, functionally graded nanocomposite coatings. *Wear,* 1999, no. 225-229, p. 65-73.

[24] STUDENÝ, Z., HRUBÝ, V., SVOBODA, E. and KUSMIC, D. Surface topology and chemical analysis of hydroxyapatite coatings enriched with AgNO3K. *Layers and Coatings 2012*. Roznov pod Radhostem, 2012, p. 115-120.

[25] CHU, K., LU, YH. and SHEN, YG. Structural and mechanical properties of titanium and titanium diboride monolayers and Ti/TiB2 multilayers. *Thin Solid Films*, 2008, vol. 516, p. 5313-5317.


## Acknowledgements

This work was financially supported under the Slovak Grant Agency under the grants VEGA 1/1103/11, 1/1102/11, 1/0279/11, 1/0264/11, 1/0108/11 and APVV-0520-10, APVV-0548-07, APVV-0682-11 and LPP-0149-09.